

A “Post-Mortem” Investigation of Cell-Level Degradation in Field SHJ Modules

Simon M.F. Zhang¹, Dana B. Sulas-Kern², Robert (μRob) Lee Chin¹, Michael E. Pollard¹, Arman Mahboubi Soufiani¹, Dirk C. Jordan², Helio R. Moutinho², Ivan Perez-Wurfl¹ and Ziv Hameiri¹

¹ University of New South Wales (UNSW), Sydney NSW 2052, Australia

² National Renewable Energy Laboratory, Golden, CO, U.S.A.

Introduction

One of most critical requirements of any photovoltaic (PV) module technology is to be reliable over its warranted lifetime. In addition, improving module reliability and extending lifetime is an especially powerful path in reducing the cost of PV systems, as it acts as a multiplier for any concurrent cost reductions [1]. To ensure reliability, detailed analyses of the long-term performance of PV systems are indispensable. This has often been done by means of continual monitoring and thorough examination of modules during and after field operation [2]–[6]. However, it seems that deeper investigations into the failure and degradation mechanisms are rarely found in the literature, especially for high efficiency technologies which are relatively new to the mass market such as silicon (Si) heterojunction (SHJ).

Despite the prominent interest in SHJ technology from both academic [7], [8] and industrial [9] sectors, there is only limited research available on the topic of SHJ module field degradation [2]–[6], and none at the cell level. Arguably the most influential study on SHJ module degradation was published recently by Jordan *et al.* [6], based on a thoroughly characterised five-module system installed in 2007 and disassembled after a *decade* of field operation. They reported that the degradation was dominated by a non-linear decrease in open-circuit voltage (V_{oc}). Subsequent studies [10], [11] identified an increase in both cell series resistance (R_s) and first-diode dark saturation current density (J_{01}). The authors suggested degradation of the transparent conductive oxide (TCO) as a possible cause for R_s increase, and surface passivation degradation in the hydrogenated amorphous silicon (a-Si:H) layers, as a cause for the increase of J_{01} .

In this study, we first present a “post-mortem” procedure for characterising cells extracted from PV modules. This procedure is then applied to the SHJ modules investigated by Jordan *et al.*, with the aim of gaining more insights regarding the observed degradation.

Methodology

Four cell fragments were extracted via coring from modules investigated in [6], three from a field-degraded module (named F1, F2, F3) and one from a module used as control (C1). The details of the coring procedure are available in [12]. C1 is used as a baseline for the degraded samples. Through preliminary testing using photoluminescence (PL) imaging, shown in Fig.1, it was determined that F1 is a relatively well-performing area of a degraded cell, whereas F2 and F3 both appear to be more adversely affected by degradation.

Besides PL imaging, the characterisation techniques used to examine the samples include quantum efficiency (QE) and micro-PL spectroscopy (μ PL). For the QE measurements, a calibrated Si detector is used in the spectral range 300 – 1000 nm and a germanium (Ge) detector is used for 1000 – 1200 nm. A Perkin Elmer 1050 spectrophotometer with integrating sphere accessory is used to conduct reflectance measurements to enable internal quantum efficiency (IQE) calculation. The spectral μ PL measurements are conducted at 30K (unless otherwise stated) using a liquid helium cryostat to control the sample temperature. A 532 nm pulsed laser, attenuated to approximately 0.4 mW and an indium gallium arsenide (InGaAs) spectrometer with sensitivity in the range 0.78 – 1.38 eV are used for optical excitation and detection, respectively.

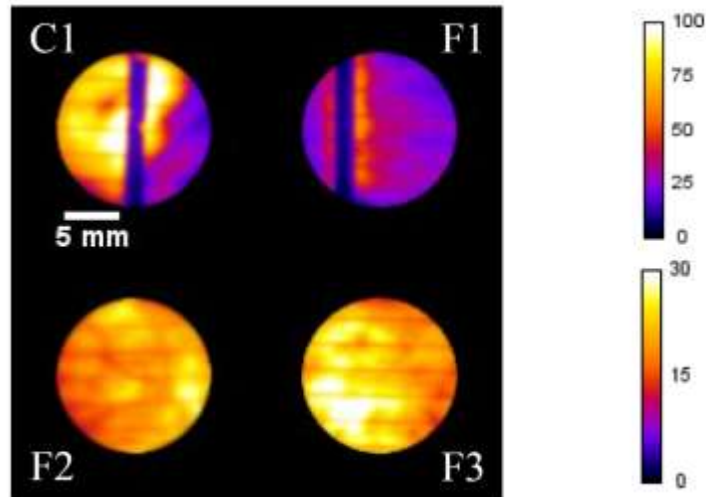


Figure 1. PL images of all samples. C1 was extracted from the control module, and F1, F2, F3 the fielded module. The colour bars indicate PL signal counts in arbitrary units. The mean brightness in the darker regions of F1 is approximately 27 AU, and the mean brightness in F2 and F3 is approximately 17 AU

Results and Discussion

Figure 2 shows the IQE for the four samples. As expected, C1 shows the highest IQE throughout the spectrum. The measurements indicate that field operation likely induces degradation in the front layers as well as in the Si bulk, as all fielded samples show degradation throughout the spectrum. Compared to C1, F1 shows the lowest amount of degradation among the field-degraded cells, verifying that it is a relatively well-performing sample. F2 shows the lowest response at wavelengths shorter than 700 nm, indicating high front passivation degradation (in combination with a possible increase of parasitic absorption), and bulk recombination. F3, on the other hand, shows the lowest long-wavelength IQE, especially within the range 900 – 1100 nm, indicating its high bulk and/or rear passivation degradation.

It should be noted that cyanoacrylate was used to mount a post to the samples during coring, and may have caused rear side damage. This may partially explain the variation in the red response. However, since the extraction process is supposedly identical, sample C1 should also suffer from this effect.

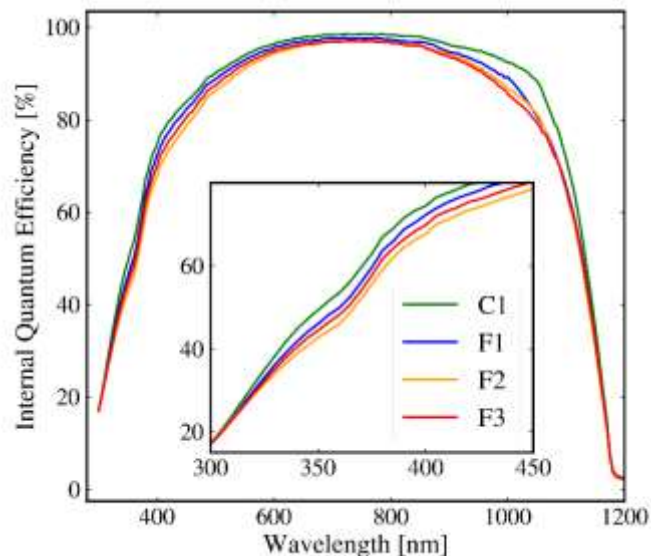


Figure 2. The internal quantum efficiency of all samples. Inset shows the blue end (300-450 nm) of the spectrum in more detail

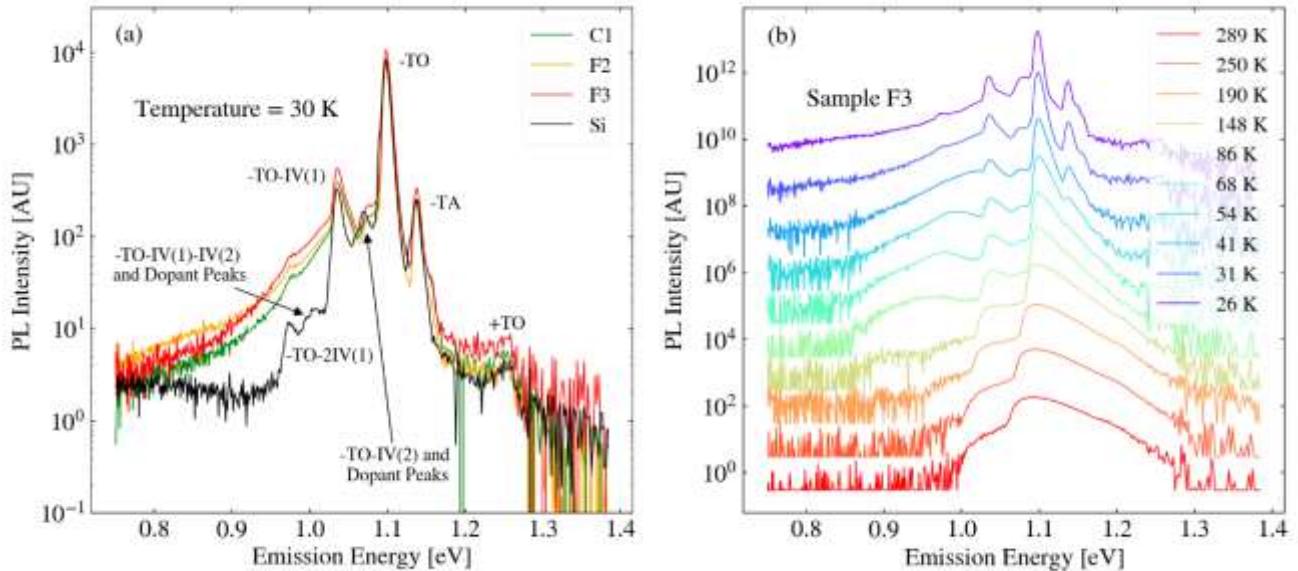


Figure 3. (a) μ PL spectra of samples C1, F2, F3 (F1 could not establish adequate thermal contact), and a Si reference sample at approximately 30 K. “+” and “-” signs indicate the absorption or emission of phonons, and “TO” and “TA” stand for “transverse optical” and “transverse acoustic” respectively. The identification of crystalline silicon band-to-band and dopant peaks is according to [13], [14]; (b) temperature-dependent μ PL spectra of sample F3. A filtering function was applied to limit the lower bound of the data to avoid clutter

Fig. 3(a) shows the μ PL spectra of SHJ samples C1, F2, F3, as well as an n-type float-zone (FZ) oxide-passivated Si wafer, at the low temperature of 30 K. Comparing to the FZ Si sample, all SHJ spectra show an additional feature between approximately 0.8 eV and 1.05 eV. One of our main aims in performing the μ PL measurements is to investigate possible degradation in the a-Si:H layers, as PL emission originating from a-Si:H was previously reported [15]. The 0.8 eV to 1.05 eV feature, being the only notable difference between the cell and wafer spectra, may be emitted from the a-Si:H layers of the SHJ cells. It is worth noting that the approximately 10 nm a-Si:H layer on either side of the cells are not expected to emit a large amount of PL signal, and that this feature may also result from other layers or mechanisms in the SHJ pieces which are absent in the silicon wafer. This feature exhibits a strong thermal quenching effect, as shown in Fig. 3(b), disappearing as temperature increases from 26 K to 54 K. After 54 K, the 0.8 eV to 1.05 eV feature gives way to another peak at 0.95 - 1.0 eV which also reduces and red-shifts as temperature increases. This is consistent with donor-acceptor pair recombination (DAP), and has been previously associated with the Si D4 dislocation line [16]. This claim requires additional investigation however, as the source of the dislocation is not apparent, since these cells comprise only a-Si:H and CZ monocrystalline Si layers.

Fig 3. (a) shows that there is no significant difference in the PL spectra among the SHJ samples. Since no significant change is seen between the degraded and non-degraded samples, to our level of sensitivity, we cannot confirm that any degradation has taken place in the a-Si:H layers of the SHJ cells.

Conclusions

We performed a post-mortem examination of cell fragments extracted from SHJ modules to characterise field degradation. We compare a range of degraded samples, as well as a control sample, using a large suite of characterisation techniques. We find that field degradation likely causes front passivation degradation and an increase in bulk defects. We present a set of μ PL measurement of SHJ cells conducted at 30 K. However, at our level of sensitivity, we do not identify a significant change in the PL signal traceable to a-Si:H degradation.

References

- [1] M. Woodhouse et al., "On the path to SunShot: the role of advancements in solar photovoltaic efficiency, reliability, and costs", National Renewable Energy Laboratory, Golden, CO, USA, 2016.
- [2] W. Luo et al., "Analysis of the long-term performance degradation of crystalline silicon photovoltaic modules in tropical climates", *IEEE J. Photovoltaics*, vol. 9, no. 1, pp. 266–271, 2019..
- [3] T. Ishii and A. Masuda, "Annual degradation rates of recent crystalline silicon photovoltaic modules", *Prog. Photovoltaics Res. Appl.*, vol. 25, no. 12, pp. 953–967, 2017.
- [4] J. Y. Ye, T. Reindl, A. G. Aberle, and T. M. Walsh, "Performance degradation of various PV module technologies in tropical Singapore", *IEEE J. Photovoltaics*, vol. 4, no. 5, pp. 1288–1294, 2014.
- [5] V. Sharma, O. S. Sastry, A. Kumar, B. Bora, and S. S. Chandel, "Degradation analysis of a-Si, (HIT) hetero-junction intrinsic thin layer silicon and m-C-Si solar photovoltaic technologies under outdoor conditions", *Energy*, vol. 72, pp. 536–546, 2014.
- [6] D. C. Jordan et al., "Silicon heterojunction system field performance", *IEEE J. Photovoltaics*, vol. 8, no. 1, pp. 177–182, 2018.
- [7] M. A. Green, "Photovoltaic technology and visions for the future", *Prog. Energy*, vol. 1, no. 1, pp. 1–13, 2019.
- [8] K. Yamamoto, K. Yoshikawa, H. Uzu, and D. Adachi, "High-efficiency heterojunction crystalline Si solar cells", *Jpn. J. Appl. Phys.*, vol. 57, no. 8, 08RB20, 2018.
- [9] "International technology roadmap for photovoltaic (ITRPV)", 2019.
- [10] D. B. Sulas, S. Johnston, and D. C. Jordan, "Comparison of photovoltaic module luminescence imaging techniques: assessing the influence of lateral currents in high-efficiency device structures", *Sol. Energy Mater. Sol. Cells*, vol. 192, pp. 81–87, 2019.
- [11] D. B. Sulas, S. Johnston, and D. C. Jordan, "Imaging lateral drift kinetics to understand causes of outdoor degradation in silicon heterojunction photovoltaic modules", *Sol. RRL*, vol. 3, no. 8, p. 1900102, 2019.
- [12] H. R. Moutinho et al., "Development of coring procedures applied to Si, CdTe, and CIGS solar panels", *Sol. Energy*, vol. 161, no. January, pp. 235–241, 2018.
- [13] D. Macdonald, A. Liu, H. T. Nguyen, S. Y. Lim, and F. E. Rougieux, "Physical modelling of luminescence spectra from crystalline silicon," in *31st European Photovoltaic Solar Energy Conference and Exhibition*, pp. 440–443, 2015.
- [14] A. Y. Liu, H. T. Nguyen, and D. Macdonald, "Quantifying boron and phosphorous dopant concentrations in silicon from photoluminescence spectroscopy at 79 K," *Phys. Status Solidi Appl. Mater. Sci.*, vol. 213, no. 11, pp. 3029–3032, 2016.
- [15] H. T. Nguyen et al., "Characterizing amorphous silicon, silicon nitride, and diffused layers in crystalline silicon solar cells using micro-photoluminescence spectroscopy", *Sol. Energy Mater. Sol. Cells*, vol. 145, pp. 403–411, 2016.
- [16] R.L. Chin, M. Pollard, Y. Zhu, and Z. Hameiri, "Detailed analysis of radiative transitions from defects in n-type monocrystalline silicon using temperature- and light intensity-dependent spectral Photoluminescence," *Sol. Energy Mater. Sol. Cells*, vol. 208, no. January, 110376, 2020.